Multiple cutout optimization in composite plates using evolutionary structural optimization

Brian G. Falzon †

*Department of Aeronautics, Imperial College of Science, Technology and Medicine,
Prince Consort Road, London, SW7 2BY, U.K.*

Grant P. Steven ‡

Department of Aeronautical Engineering, University of Sydney, Sydney, N.S.W. 2006, Australia

Mike Y. Xie ‡†

*Department of Civil and Building Engineering, Victoria University of Technology,
Melbourne, VIC. 8001, Australia*

Abstract. The optimization of cutouts in composite plates was investigated by implementing a procedure known as Evolutionary Structural Optimization. Perforations were introduced into a finite element mesh of the plate from which one or more cutouts of a predetermined size were evolved. In the examples presented, plates were rejected from around each evolving cutout based on a predefined rejection criterion. The limiting ply within each plate element around the cutout was determined based on the Tsai-Hill failure criterion. Finite element plates with values below the product of the average Tsai-Hill number and a rejection criterion were subsequently removed. This process was iterated until a steady state was reached and the rejection criterion was then incremented by an evolutionary rate and the above steps repeated until the desired cutout area was achieved. Various plates with differing lay-up and loading parameters were investigated to demonstrate the generality and robustness of this optimization procedure.

Key words: composite plates; optimization; evolutionary structural optimization; cutouts; failure criterion; biaxial; shear.

1. Introduction

The use of cutouts in aerostructures introduces areas of stress concentrations which may limit the operational life of an aircraft. The emergence of carbon fibre composite technology has allowed aircraft designers to not only design the aerostructure itself but to also design the material to best serve the prescribed function. This has meant that, in theory, the innovative placement of composite layers around a cutout could reduce the stress concentrations normally expected

---

† Research Associate
‡ Professor
‡† Senior Lecturer

from the use of isotropic materials. Lin and Lee (1992) adopted a fibre placement technique to optimize the strength of a glass fibre panel containing a circular hole while Hyer and Lee (1991) used this method to optimize the buckling strength of composite panels with a circular hole.

In practice, manufacturing limitations prevent this method from being effectively applied to large complex structures such as a fuselage or a wing. Often the ply orientations making up a required laminate are determined by strength and aeroelastic considerations and the introduced cutouts are reinforced appropriately to diffuse the stress concentrations around these regions. Where the cutouts are required to be of a specific shape and size, reinforcement may be the only option available to the designer. Recently Senocak and Waas (1995) presented a numerical method whereby a reinforcement of varying sectional area was produced such that the presence of the hole did not alter the prevailing stress field.

In some cases, such as the introduction of lightening holes or access panels, there may be scope for variations in the shape of the cutout. It is then possible to chose a cutout shape, within an existing laminate, that would give rise to the least perturbation in the stress field. This class of problems has been addressed through various shape optimisation schemes. Bäcklund and Isby (1988) used a point stress criterion at a characteristic distance of 1 mm from the hole's edge along with a Tsai-Hill failure index to determine the stress field in the vicinity of a cutout in a composite panel. The hole was defined using spline curves and these were allowed to change with the objective of minimising the weight without increasing the maximum Tsai-Hill value. Ahlstrom and Bäcklund (1992) demonstrated this procedure by optimizing cutouts in pressure vessels. Vellaichamy, et al. (1990) investigated the optimum orientation and aspect ratio of elliptical cutouts in composite structures for various lay-ups and load cases with the objective of minimising the maximum failure criterion around the hole. Han and Wang (1993) investigated the location, size and orientation of a hole in a plate by minimising the maximum tangential strain energy along the hole boundary. This was achieved by formulating the above as a linear programming problem coupled with finite element capability.

Xie and Steven (1993) developed a simple evolutionary procedure for structural and layout optimization and termed it Evolutionary Structural Optimization (ESO). This method has the advantage of being conceptually intuitive and the developed optimization routines are easily incorporated into existing finite element packages. The essence of this procedure, applied to shape optimization, is to remove parts of the structure which are in a state of low stress, subject to a pre-defined rejection criterion, until an optimized shape is evolved. Xie and Steven (1994a) have successfully demonstrated the applicability of ESO to the optimization of structures for multiple load cases by comparison with existing solutions. This work was subsequently extended by Steven, et al. (1995) to include multiple support conditions. The frequency optimization of structures using this evolutionary procedure was also investigated by Xie and Steven (1994b).

The authors have extended this Evolutionary Structural Optimization procedure to optimize the shape of multiple cutouts in a composite plate of arbitrary lay-up. A rejection criterion, using a layerwise approach and first-ply-failure philosophy, was adopted in removing elements on the interior edge of each cutout and this is explained in some detail in the following section. Through various examples presented it will be shown that a reduction in maximum stresses was always achieved using ESO.
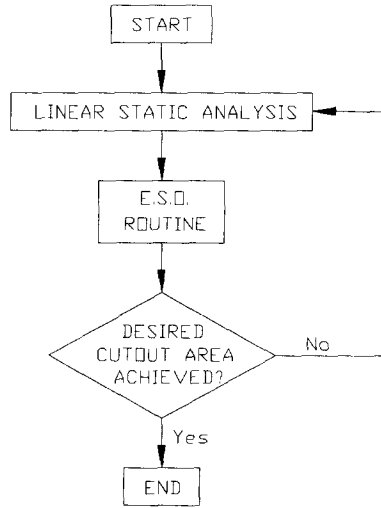
Fig. 1 Optimization flowchart.

2. Evolutionary structural optimization

Evolutionary Structural Optimization is an attempt to simulate evolution, as observed in nature, through the use of numerical methods. This method has now been extended to include the optimization of cutouts in composite structures. Using Finite Element Analysis, a plate was modelled with one or more small interior cutouts to be optimized and the stress distribution was calculated from a linear static analysis resulting from a pre-defined loading. A failure criterion number was assigned to each composite layer within each element. By adopting a first-ply-failure philosophy, the ply with the maximum failure criterion number within each plate on the interior free edges was chosen as the limiting ply for the plate element.

A failure criterion is used to predict the onset of damage within a laminate and provides no information on the damage growth or the extent of degradation within a laminate once this criterion is exceeded. By incorporating a first-ply-failure philosophy, the assumption is made that the whole laminate is limited by the strength of the weakest layer. The criterion chosen in this study was the Tsai-Hill failure criterion:

$$\left(\frac{\sigma_1}{X}\right)^2 + \left(\frac{\sigma_2}{Y}\right)^2 - \sigma_1\sigma_2\left(\frac{1}{X^2} + \frac{1}{Y^2}\right) + \left(\frac{\tau_{12}}{S}\right)^2 \geq 1 \tag{1}$$

where σ_1 and σ_2 are the stresses in the fibre and transverse directions respectively, τ_{12} the shear stress and X, Y and S are the corresponding strengths which will have different values for tension and compression.

Once the limiting ply for each plate element on the interior of a free edge of a particular cutout was determined, plates were rejected from this edge, subject to a user-specified rejection criterion. This rejection criterion was chosen such that an element was rejected if its representative failure index was less than the product of the user-specified rejection ratio (*RR*) and the average Tsai-Hill number of all the plates in the finite element model:

$$REJECT\ PLATE\ e{\in}E\ \ if\ \ TH(e) < \frac{1}{P}\sum_{p=1}^{P}\ TH(p){\times}RR \tag{2}$$

where $TH(e)$ is the limiting Tsai-Hill value of element e lying on the edge of a cutout, E is the set of all element lying on the edge of the cutout, P is the total number of plates in the FE model and $TH(p)$ is the limiting Tsai-Hill value of plate element $p \in P$. It follows that $E \subset P$. The linear static analysis was repeated for the updated structure using the same rejection ratio until a steady state was reached, i.e., when no more plates were rejected. The rejection ratio was then updated by an evolutionary rate (ER) also specified by the user:

$$RR_{i+1} = RR_i + ER \tag{3}$$

where the subscript i refers to the increment number. This process was repeated until a cutout of a desired area was achieved. The simplified flow chart in Fig. 1 shows how the ESO module, which was written as a FORTRAN code, was utilised along with a commercial finite element analysis package, STRAND6 (1993), in optimising cutouts in composite structures.

3. Results and discussion

Various example of the optimization of one or more cutouts in composite panels with different lay-ups and loading conditions are presented which demonstrate the generality of this procedure. The objective of introducing an optimally shaped cutout is to minimise its influence on the overall structure. One way to measure this improvement was to record the change in maximum Tsai-Hill number around the cutout through its evolutionary history and to compare this value with that of a non-optimized cutout with an equivalent area. Any cutout shape which deviated from the ideal optimized one may be classed as non-optimized although in the examples presented, the non-optimized cutout shape was defined by the initial cutout shape on which the optimization proceeded unless otherwise stated. In further assessing the optimality of the resulting cutout, the standard deviation, s, of the representative Tsai-Hill numbers of all the plates on the edge of the cutout was recorded and compared with that obtained from the non-optimized case. Whereas the first measurement concerned a localised phenomenon, the second pertained to the whole cutout boundary and a lower standard deviation implied less variability between the distribution of maximum and minimum Tsai-Hill values about the mean Tsai-Hill value in this region. This, in turn, suggested that the material around the interior free edge was being used more effectively as the shape of the cutout was evolved.

Graphs of the evolutionary history are presented for each example which provide a history

Table 1 Material data

Nominal material data for unidirectional carbon fibre composite		
E_1	128 GPa	
E_2	11.3 GPa	
G_{12}	6.0 GPa	
μ_{12}	0.3	
Ply thickness	0.16 mm	
STRENGTH	TENSILE	COMPRESSIVE
Longitudinal	1.45 GPa	1.25 GPa
Transverse	52 MPa	100 MPa
Shear	93 MPa	

of the maximum, minimum, mean and standard deviation around the interior free edge. Where more than one cutout was introduced, these graphs were observed to be identical for each cutout and only one has been included. Non-optimized values are shown in solid symbols at the last evolution index and the pertinent data has been tabulated showing percentage differences with respect to the non-optimized values. A global mean Tsai-Hill number is given for the first three examples although, as expected, this value remains fairly constant. In each case the applied loading has been scaled such that the maximum non-optimized Tsai-Hill value corresponded to unity. Nominal material values for unidirectional carbon fibre composite are listed in Table 1.

3.1. Example 1: Quasi-isotropic $[\pm 45/0/90]_s$ plate loaded in biaxial tension

An equibiaxial stress and a 2:1 biaxial stress ratio were each, in turn applied to a square quasi-isotropic plate. The original meshes, showing the applied stresses in each case are shown in Fig. 2.

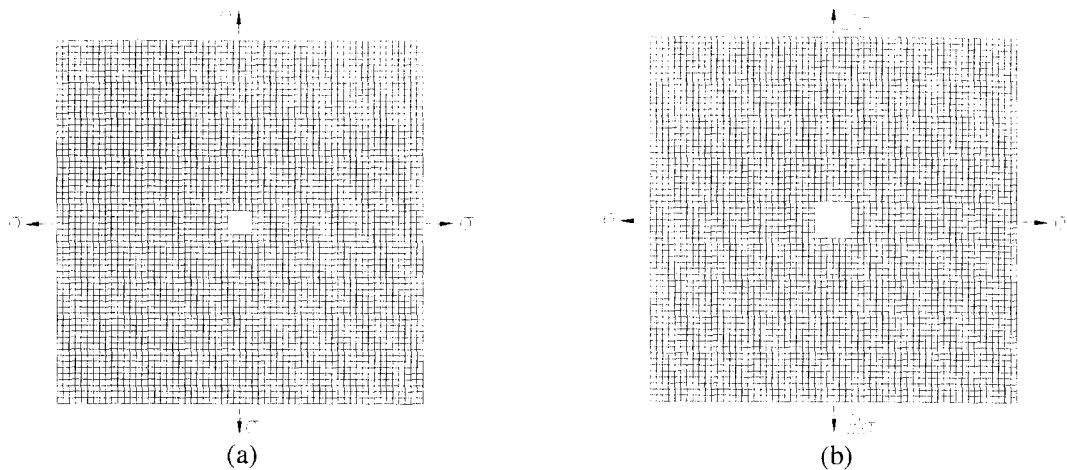(a)   (b)

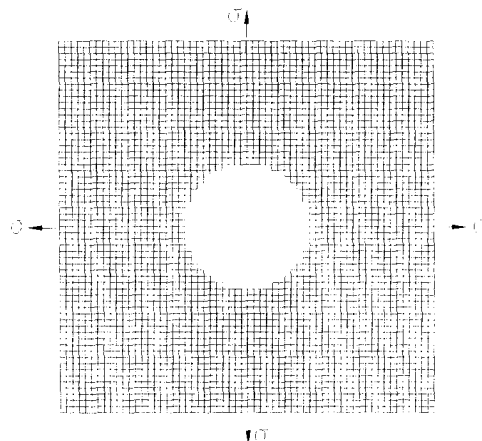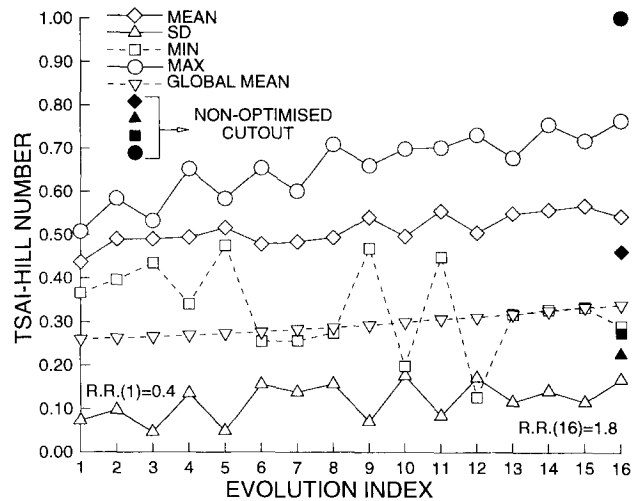Fig. 2 Initial cutout in a $[\pm 45/0/90]_s$ plate in (a) equibiaxial stress state; (b) 2:1 biaxial stress ratio.

Fig. 3 Optimized cutout in a $[\pm 45/0/90]_s$ plate loaded in equibiaxial stress.

	Opt.	Non-Opt.	% diff.
$TH(e)_{max}$	0.76	1.0	24
s	0.17	0.28	39

Fig. 4 Evolutionary history of a $[\pm 45/0/90]_s$ plate loaded in equibiaxial stress.
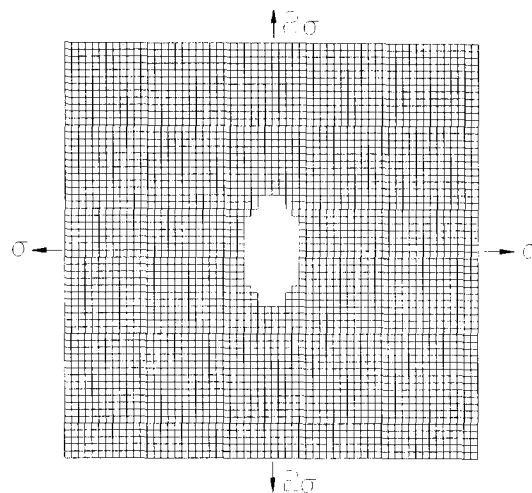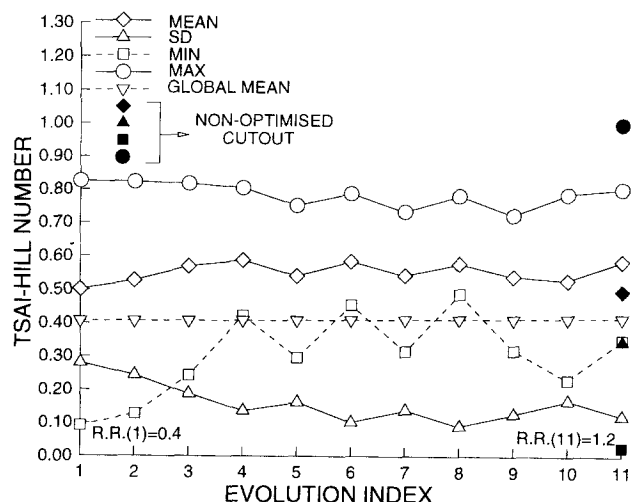

Fig. 5 Optimized cutout in a $[\pm 45/0/90]_s$ plate loaded in (2:1) biaxial stress.

The resulting optimized cutout, shown in Fig. 3, for the equibiaxial stress state was a circle and this corresponded to the shape expected from an isotropic plate under identical loading conditions. The percentage reductions with respect to the non-optimized cutout were 24% in $TH(e)_{max}$ and 39% in s. Fig. 4 shows the history of the cutout s evolution. The gradual increase in $TH(e)_{max}$ was due to the inevitable increase in energy density of the system as more material was removed from the panel of finite dimensions.

In the case of a 2:1 biaxial stress ratio, where the longitudinal stress was double that in

	Opt.	Non-Opt.	% diff.
$TH(e)_{max}$	0.8	1.0	20
s	0.12	0.35	66

Fig. 6 Evolutionary history of a $[\pm 45/0/90]_s$ plate loaded in (2:1) biaxial stress.

the transverse direction, the optimized cutout closely resembled an ellipse of aspect ratio (AR) 2 and is shown in Fig. 5. The corresponding evolutionary history is given in Fig. 6. As will be shown this result is analogous to that of an isotropic plate. For an infinite isotropic plate in a biaxial stress state and containing an elliptical cutout oriented such that its major axis are parallel to the panel's longitudinal axis, the stress at the vertices may be expressed as, Lekhnits-kii (1968):

$$\sigma_A = \sigma_1\left(1 + 2\frac{a}{b}\right) - \sigma_2$$

$$\sigma_B = \sigma_2\left(1 + 2\frac{a}{b}\right) - \sigma_1 \tag{4}$$

where σ_A and σ_B are the stresses at the major and minor vertices of the ellipse respectively, and a and b the major and minor elliptical axes. If the plate is in an equibiaxial stress field ($\sigma_1 = \sigma_2$) and by defining an optimum stress distribution as being one where $\sigma_A = \sigma_B$, then by substituting these relations into Eq. (4) we find that the optimum shape which achieves this stress state is a circle ($a = b$) as was indeed obtained through the optimization procedure for the quasi-isotropic plate. If the applied stress ratio is 2:1, by maintaining the assumption that an optimum shape is one which equalises the stresses at the vertices, then an ellipse of $AR = 2$ is obtained. $TH(e)_{max}$ and s were reduced by 20% and 66% respectively.

3.2. Example 2: Quasi-isotropic [45/0/90]ₛ plate loaded in biaxial and shear stress

In this example a shear stress component τ, was introduced to further validate the generality
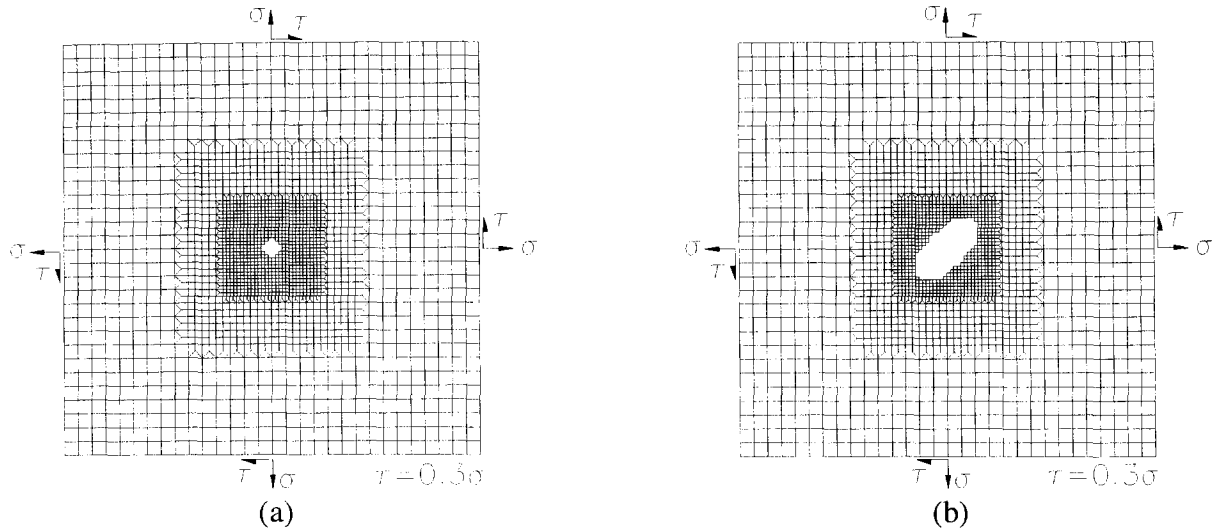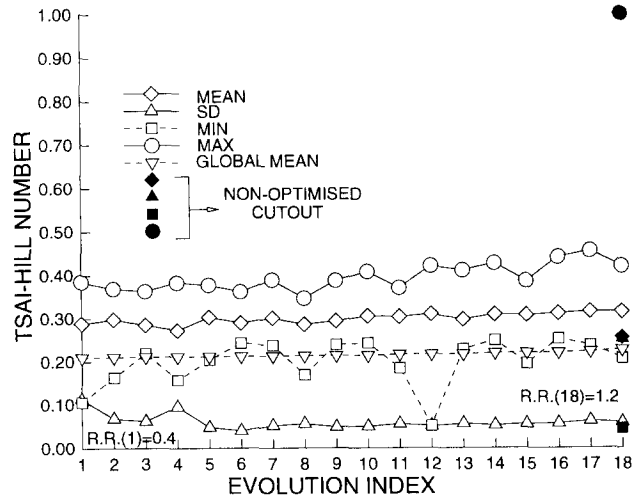
Fig. 7 [± 45/0/90]$_s$ Plate loaded in (1:1:0.3) biaxial and shear stress; (a) Initial cutout, (b) Optimized cutout.

	Opt.	Non-Opt.	% diff.
$TH(e)_{max}$	0.46	1.0	54
s	0.06	0.25	76

Fig. 8 Evolutionary history of a [± 45/0/90]$_s$ plate loaded in (1:1:0.3) biaxial and shear stress.

of this optimization procedure. Various ratios of shear stress to axial stress were investigated and in all cases the optimized cutout was an ellipse oriented at 45° with varying aspect ratio. Fig. 7 shows the starting mesh and the final optimized cutout, with an $AR = 2.04$, for the case when $\tau = 0.3\sigma$. Two other τ ratios where investigated; $\tau = \sigma$ and $\tau = 0.6\sigma$. The optimized shape for $\tau = \sigma$ was a slit with a high, but finite, aspect ratio defined by the width of the initial cutout.

The aspect ratio for the $\tau = 0.6\sigma$ case was measured at 4.07. These values were obtained by fitting an ellipse through the cutout and measuring its axial dimensions. The evolutionary history in Fig. 8 shows fairly uniform values with increasing cutout size. This suggests that the optimal shape was reached early in the evolution history with subsequent iterations serving to further increase the size of the cutout without significant changes to its shape. $TH(e)_{max}$ and s were reduced by 54% and 76% respectively.

To verify the AR under these loading conditions, reference is again made to the isotropic case. By constructing a Mohr Circle and expressing·the shear stress as a function of the axial stress it may be easily shown that the principal stresses are orientated at 45° corresponding to the orientation of the optimum ellipse's axes and with the major axis in the direction of the maximum principal stress. In an infinite isotropic plate under equibiaxial stress F and shear stress $F\tau$, where $0 \le F \le 1$ and $\sigma = \tau$, it can be easily shown by again invoking Eq. (4), that the optimum aspect ratio for the ellipse may be expressed as:

$$AR = \frac{a}{b} = \frac{1+F}{1-F} \qquad (5)$$

Table 2 provides a comparison of the aspect ratios of the various optimised cutouts with those obtained from the above analysis applied to an isotropic plate.

3.3. Example 3: Quasi-isotropic $[45/0/90]_s$ and angle-ply $[(\pm 30)_2]_s$ plates loaded in shear stress and containing two cutouts

Table 2 Comparison of elliptical aspect ratios

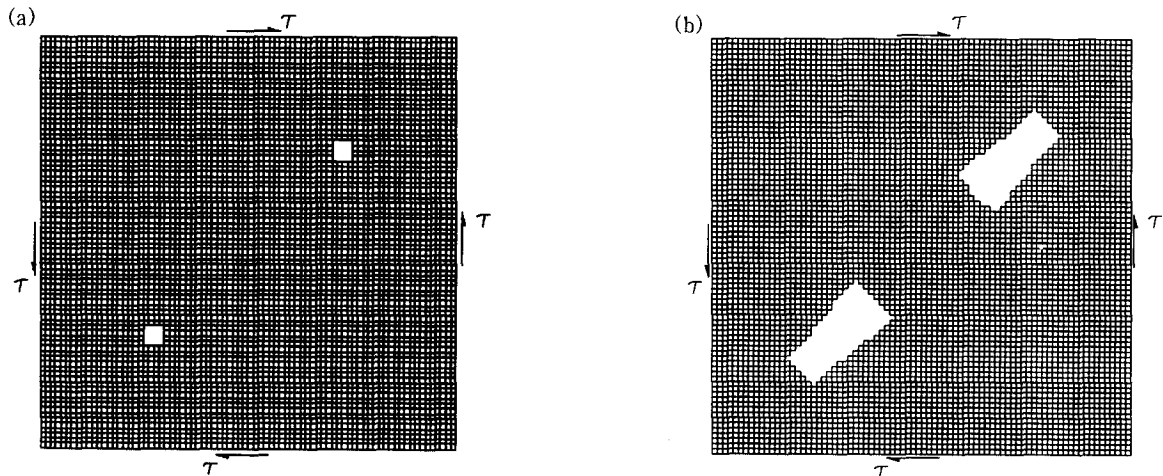| F	AR (ESO)	AR (analysis)
1.0	Slit	∞
0.6	4.07	4.00
0.3	2.04	1.86

Fig. 9 $[\pm 45/0/90]_s$ Plate loaded in shear and containing two cutouts: (a) Initial cutouts, (b) Optimized cutouts.

In the following examples the optimization of two holes in a plate loaded in pure shear was investigated. Two plates, one with a quasi-isotropic lay-up of $[\pm 45/0/90]_s$, and the other with an angly-ply lay-up of $[(\pm 30)_2]_s$, are presented. The cutouts were evolved from two perforations with their centres at x-y coordinates $(0.25L, 0.25L)$ and $(0.75L, 0.75L)$ where L is the length of the side of the square plate and the global axis system is assumed to have its origin at the bottom left corner of the plate.

Fig. 9 shows the initial and optimized cutouts for the quasi-isotropic plate. The cutouts are trapezoidal as opposed to rectangular as was observed by Falzon (1995) for a single centrally
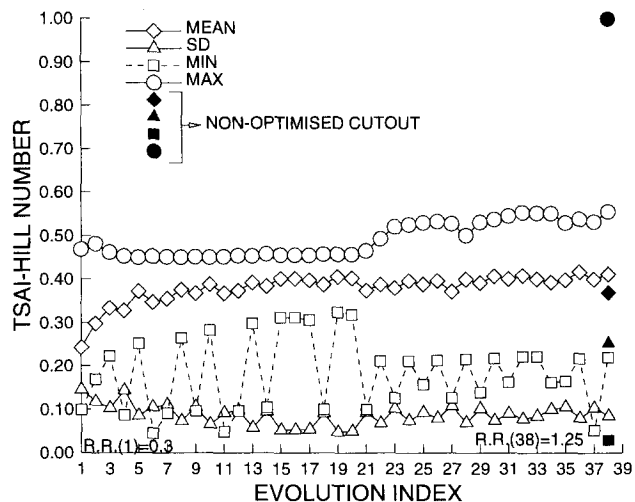
	Opt.	Non-Opt.	% diff.
$TH(e)_{max}$	0.56	1.0	44
s	0.08	0.25	68

Fig. 10 Evolutionary history of a $[\pm 45/0/90]_s$ plate loaded in shear and containing two cutouts.
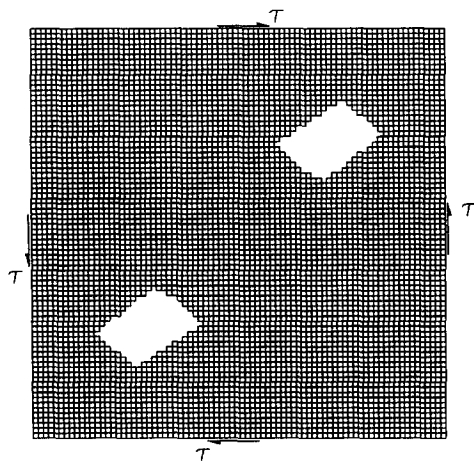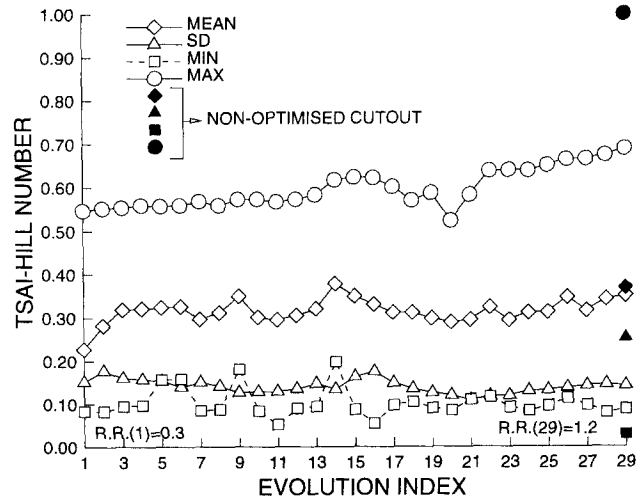

Fig. 11 $[(\pm 30)_2]_s$ Plate loaded in shear and containing two optimized cutouts.

located cutout in an identical plate and loading configuration. These cutouts may then be viewed as being basically rectangular but with a tapering arising from the edge effects. The evolutionary history for this example is given in Fig. 10 which also shows significant reductions in the maximum Tsai-Hill value and in the standard deviation of the values at the edge of each cutout. $TH(e)_{max}$ and s were reduced by 44% and 68% respectively. For this and subsequent examples, the non-optimised cutouts were asssumed to be circular and having the same area as the optimized ones.

Fig. 11 shows the optimized cutouts in an angle-ply laminate with a lay-up of $[(\pm 30)_2]_s$ and also loaded in shear. The aspect ratio of these cutouts was less than that of the preceeding example. It is interesting to note that whereas the cutouts in the quasi-isotropic case were mirror images of each other about the separating diagonal of the plate, the cutouts in the present case were such that the mirrored image was also rotated 180 about the other (bisecting) diagonal. The evolutionary history is given in Fig. 12 and shows a reduction of 31% in $TH(e)_{max}$ and 50% in s.

3.4. Example 4: Quasi-isotropic $[\pm 45/0/90]_s$ and angle-ply $[(\pm 30)_2]_s$ plates loaded in biaxial and shear stress and containing four cutouts

Fig. 13 shows the resulting optimized elliptical cutouts for a quasi-isotropic plate loaded in biaxial and shear. The shape, orientation and aspect ratio of these cutouts closely resembled the optimized shape of a centrally located single cutout in an identical plate (cf. Fig. 7). The evolutionary history shown in Fig. 14 shows an increasing value of $TH(e)_{max}$ beyond the 19th iteration. This increase was alluded to earlier as being due to the inevitable increase in energy density of the system as more material was removed from the panel of finite dimensions. The

	Opt.	Non-Opt.	% diff.
$TH(e)_{max}$	0.69	1.0	31
s	0.14	0.28	50

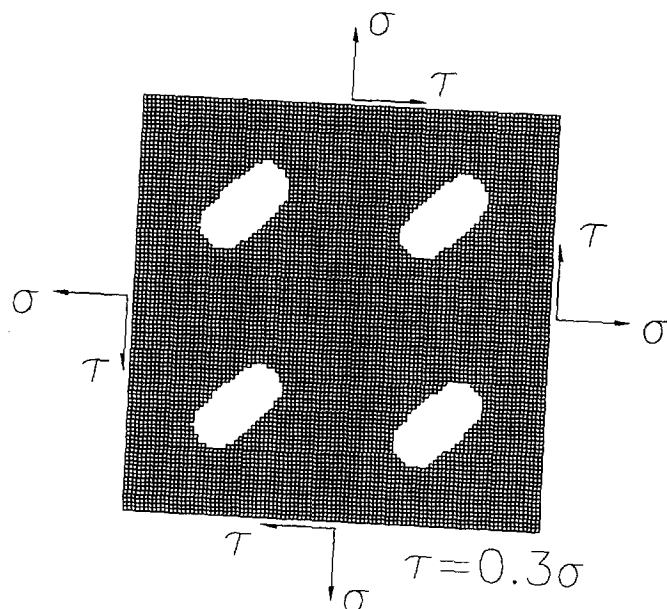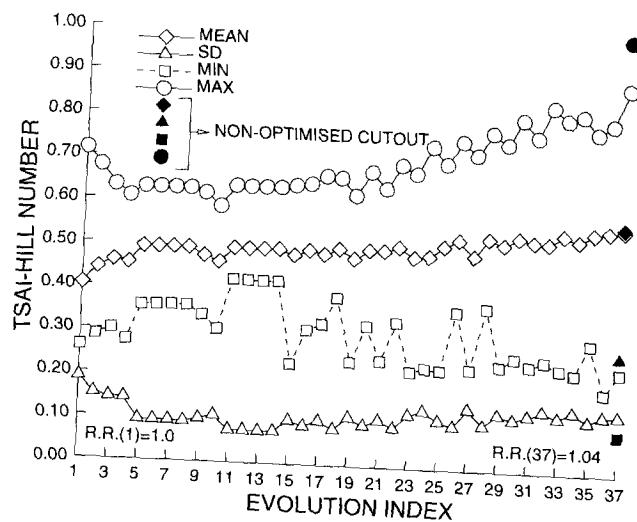Fig. 12 Evolutionary history of a $[(\pm 30)_2]_s$ plate loaded in shear and containing two cutouts.

Fig. 13 Optimized cutouts in a $[\pm 45/0/90]_s$ plate loaded in equibiaxal and shear.

	Opt.	Non-Opt.	% diff.
$TH(e)_{max}$	0.89	1.0	11
s	0.14	0.27	48

Fig. 14 Evolutionary history of a $[\pm 45/0/90]_s$ plate loaded in biaxial and shear and containing four cutouts.

standard deviation values beyond the 19th iteration remained fairly uniform implying that the subsequent removal of material beyond this point was achieved without degrading the distribution of stresses around the hole. Hence, while the reduction in $TH(e)_{max}$ was only 11% over that
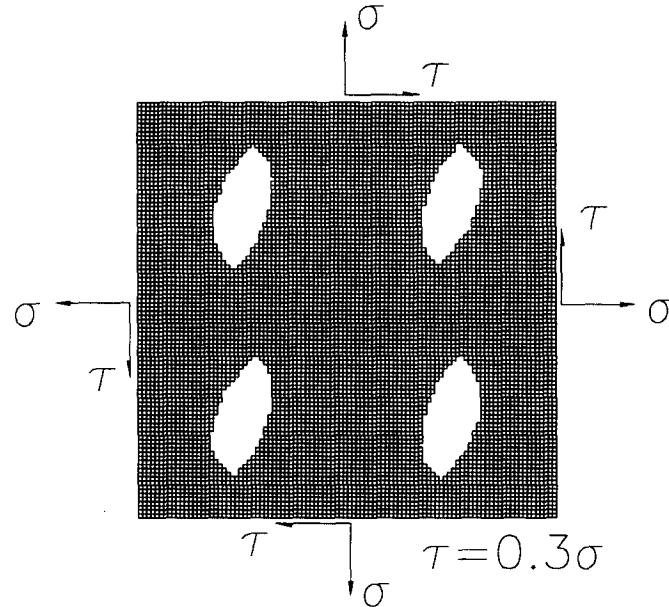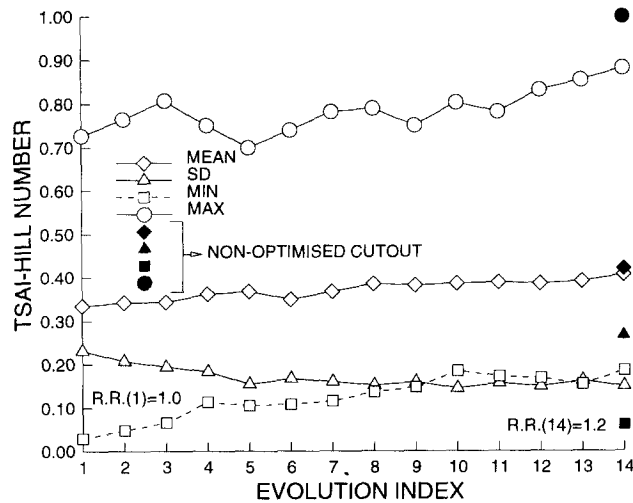
Fig. 15 Optimized cutouts in a $[(\pm 30)_2]_s$ plate loaded in equibiaxial and shear.

	Opt.	Non-Opt.	% diff.
$TH(e)_{max}$	0.89	1.0	11
s	0.15	0.26	42

Fig. 16 Evolutionary history of a $[(\pm 30)_2]_s$ plate loaded in biaxial and shear and containing four cutouts.

obtained from a plate with four circular cutouts of the same area, the reduction in s was 48%.

The optimized cutouts in the angle-ply laminate resembled the shape of a leaf and are shown in Fig. 15. The reduction in $TH(e)_{max}$ over the non-optimised case was 11% - the same as the preceeding example while the reduction in s was 42%. The evolutionary history in Fig. 16 again

shows an increase in $TH(e)_{max}$ with increasing cutout size.

3.5. Example 5: Cutout interaction in a quasi-isotropic plate

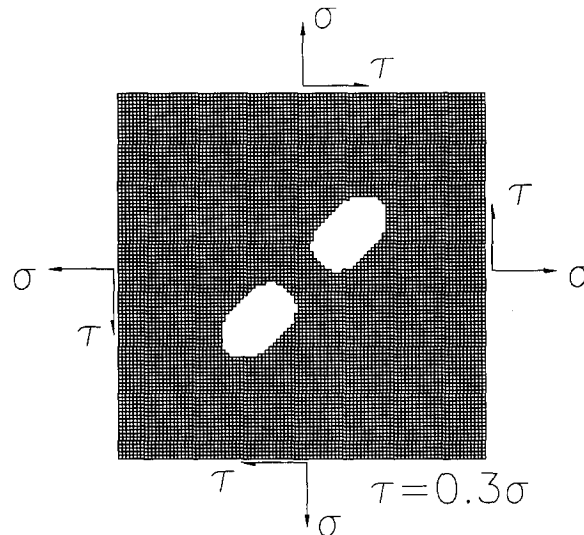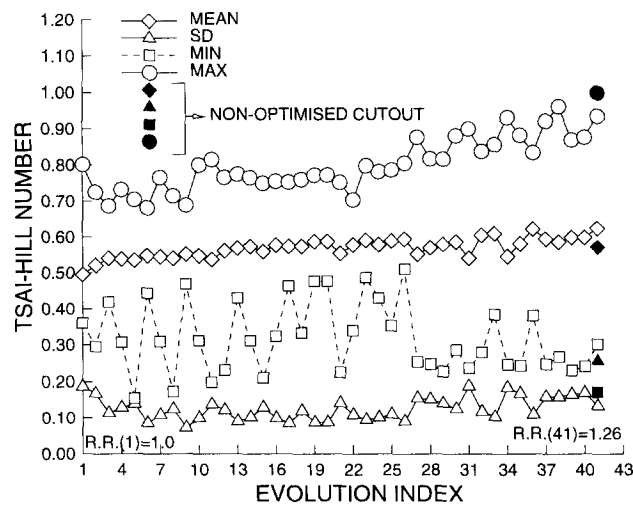In the multiple cutout problems presented so far, the cutouts have been placed far enough

Fig. 17 Cutout interaction in a $[\pm 45/0/90]_s$ plate loaded in biaxial and shear.

	Opt.	Non-Opt.	% diff.
$TH(e)_{max}$	0.94	1.0	6
s	0.14	0.26	46

Fig. 18 Evolutionary history of $[\pm 45/0/90]_s$ plate loaded in (1:1:0.3) biaxial and shear and containing two cutouts in close proximity.

apart not to influence each other. In this example, two perforations were placed at locations (0.375*L*, 0.375*L*) and (0.625*L*, 0.625*L*) in a quasi-isotropic plate with a (1:1:0.3) biaxial and shear stress loading. It is known from Example 2 that the optimized shape of a centrally located cutout in this plate is elliptical with an aspect ratio of approximately 2. This meant that for the present case, if the cutouts were to also evolve to ellipses, they would extend towards each other. This gave rise to an interaction of the stress fields around each cutout as observed in Fig. 17. The interaction of the stress fields prevented each cutout from evolving into a full ellipse giving rise to the observed shapes where the ends of each cutout, pointing toward the centre of the plate, have been flattened in the presence of a higher stress field in this region. The evolution history in Fig. 18 shows a 6% reduction in $TH(e)_{max}$ while a reduction of 46% in s was achieved.

4. Conclusions

An Evolutionary Structural Optimization procedure for optimizing interior cutouts in composite plates has been implemented. The strength of this method lies in its intuitive simplicity and is easily incorporated into commercially available finite element packages. Plates with a varying number of cutouts, lay-up configurations and loading conditions were investigated. In all cases presented, a reduction in the maximum stress around the cutout was achieved (expressed as a Tsai-Hill number) as well as a reduction in the standard deviation of the stress values around the cutout. This procedure is not restricted to two-dimensional problems and may be easily applied to complex engineering-type structures.

References

Ahlstrom, L.M., Bäcklund, J. (1992), "Shape optimization of opening in composite pressure vessels", *Composite Structures*, **20**, 53-62.

Bäcklund, J., Isby, R. (1988), "Shape optimization of holes in composite shear panels", *Structural Optimization*, Rozvany, G.I.N., Karihaloo, B.L., Editors, pp 9-16, Kluwer Academic Publishers.

Falzon, B.G. (1995), "An investigation into the buckling and postbuckling behaviour of hat-stiffened composite panels", *PhD Thesis*, Department of Aeronautics, University of Sydney, NSW 2008, Australia.

Han, C.S., Wang, B.P. (1993), "Optimum design of rectangular panels with a hole", *Advances in Engineering Software*, **17**, 127-134.

Hyer, M.W., Lee, H.H. (1991), "The use of curvilinear fiber format to improve buckling resistance of composite plates with central circular holes", *Composite Structures*, **18**, 239-261.

Lekhnitskii, S.G. (1968), "Anisotropic plates", Gordon and Breach Science Publishers, New York.

Lin, H.J, Lee, Y.J. (1992), "Strength of composite laminates with continuous fibres around a circular hole", *Composite Structures*, **21**, 155-162.

Senocak, E., Wass, A. (1995), "Optimally reinforced cutouts in circular cylindrical shells", *Proceedings of the 36th AIAA/ASCE/ASME/AHS/ASC Structures*, Structural Dynamics and Materials Conference, New Orleans, Louisiana, 409-415, April.

STRAND6 Reference *Manual and User Guide*, G+D Computing, Sydney (1993).

Vellaichamy, S., Prakash, B.G., Brun, S. (1990), "Optimum design of cutouts in laminated composite structures", *Computers and Structures*, **37**(3), 241-246.

Xie, Y.M., Steven, G.P. (1993), "A simple evolutionary procedure for structural optimization", *Computers*

and Structures, **49**, 885-896.

Xie, Y.M., Steven, G.P. (1994a), "Optimal design of multiple load case structures using an evolutionary procedure", *Engineering Computations,* **11**, 295-302.

Xie, Y.M., Steven, G.P. (1994b), "A simple approach to structural frequency optimization", *Computers and Structures,* **53**, 1487-1491.